Optimal system configuration and operation strategies of flexible hybrid nuclear-solar power plants

Abdullah A. Al Kindi[a], Antonio M. Pantaleo[a,b], Kai Wang[a,c], Christos N. Markides[a,*]

[a] *Clean Energy Processes (CEP) Laboratory and Centre for Process Systems Engineering (CPSE), Department of Chemical Engineering, Imperial College London, London, UK*
[b] *Department of Agro-Environmetnal Sciences, University of Bari, Via Amendola 165/A, 70125 Bari, Italy*
[c] *Institute of Refrigeration and Cryogenics, Zhejiang University, Hangzhou 310027, China*
[*] *c.markides@imperial.ac.uk*, ***CA***

Abstract:

Nuclear power plants are commonly used for baseload power supply due to their high reliability, low variable costs, as well as relatively low thermal efficiencies and limited load-following capabilities; especially, in the case of light water reactors. At the same time, concentrating solar power (CSP) technology is gaining attention, but is still considered an intermittent source of power with a limited availability factor. In an effort to propose a very different performance characteristic for both technologies, a hybrid power system combining nuclear and CSP plants and integrated with a thermal energy storage system is considered in this paper. The integration of the technologies is achieved by adding an indirect solar superheater and a solar reheater to a small modular nuclear reactor (NuScale). The work includes modelling of the integrated hybrid system, thermodynamic performance analysis and operational optimization aimed at maximizing the profitability of such a hybrid power plant in Oman. The results show that the hybrid system has the potential to deliver more efficient and flexible power (operating between 55% and 100% of nominal load) with the nuclear reactor operated continuously at its full rated power. The hybridization concept can potentially produce a competitive levelized cost of electricity, especially with the integration of thermal energy storage. The study concludes that the installation of such a system in Oman is not yet economically viable unless electricity tariffs increase by 70% to UK levels.

Keywords:

Concentrated solar power, nuclear power, part-load performance, steam turbine, thermal energy storage.

1. Introduction

Nuclear Power Plants (NPPs) are commonly operated to meet the baseload electricity demand due to their high reliability, high capital costs, and relatively low variable operating costs. Although nuclear is an attractive option for energy mix decarbonization, it is not currently favoured due to increasing costs, long construction times and delays, relatively low thermal efficiency, and limited and uneconomic load-following capabilities. In response to the issues raised by the first two challenges, the nuclear industry has been shifting toward Small Modular Reactors (SMR) which are smaller, simpler, standardized and safer. SMRs are expected to offer better upfront capital cost affordability and shorter construction times [1]. Most NPPs, especially light water reactors, have thermal efficiencies ranging between 30% and 34%, which are relatively low compared to the other conventional power plants (e.g., ~40-45% for steam power plants, or ~50-60% for combined cycle gas turbines). The low efficiency levels are mainly due to temperature constraints and the need of liquid water in the reactor vessels [2].

NPPs with load-following capabilities are currently required in the energy mix due to the high penetration of renewables that compete with nuclear power in providing baseload demand [3]. However, it is not economical to run nuclear reactors at power levels below the full rated power since it takes longer times to have a positive return of investment. Several studies proposed combining NPPs with renewables (i.e., solar thermal power or wind) to create a hybrid system that allows NPPs to operate at constant full rated power. The hybrid systems manage to meet the fluctuating energy demand and utilize the excess thermal energy from the combined resources for other heat applications [4-7]. Therefore, the hybridization concept has the potential of delivering flexible power with improved NPPs capital investment return.

Concentrated Solar Power (CSP) has been a rapidly growing sector. Traditionally, key disadvantages of CSP plants arise from their high costs and dependency on variable weather conditions, which is commonly nowadays tackled by using Thermal Energy Storage (TES) that makes plants capable of storing heat for about 15 h and generating power during low or no sunlight periods. Interestingly, and although this storage period is not sufficient to ensure power in conditions when there is no sun for several days [8], it does offer CSP technology the capability to perform a range of functions, with costs decreasing significantly in the past 1-2 decades. Therefore, it remains important to investigate the options for further increasing the availability factor of CSP plants. One option is to hybridize solar with other power plants that have high availability factors such as biomass or nuclear [9,10].

A few studies have proposed combining nuclear with solar energy in hybrid nuclear-solar power systems [11,12]. A study by Popov et al. [12] showed that such a hybrid system using heat generated by CSP to superheat steam from the nuclear reactor to about 555 °C can increase the full-load efficiency of the power station by 36%, relative to a standalone nuclear reactor. Hybridizing nuclear (with its high capacity and availability factor) with solar also increases the availability factor of CSP plants. However, these studies did not consider the load-following capabilities of such systems, optimize the TES system capacity for specific locations, or the economic proposition of such plants.

Many studies have covered TES sizing, power dispatchability and control of CSP plants. Casella et al. [13] developed a model for optimal control where power dispatchability is performed at peak hours to maximize the annual profitability. Guedez et al. [14] created a methodology for maximizing profits based on electricity market prices and tariffs in South Africa by determining optimal solar-tower power plant configurations and operating strategies. Both studies concluded that, *for standalone CSP plants*, optimal control and TES sizing should be considered for aiding the decision-making at early stages of the design process, and when estimating potential project revenues.

Zhuang et al. [15] conducted a detailed economic study and calculated the Levelized Cost of Electricity (LCOE) of a 100MW tower CSP plant at different locations in China. Their study showed that CSP will become more economically competitive if incentive policy is initiated in China. Parrado et al. [16] studied the effect of learning curves on reducing the LCOE from 2014 to 2050 at different global regions. Their results showed that the current LCOE of a CSP plant has the potential to be reduced by almost 50%, which shows the potential of a highly competitive CSP power in the future.

The aim of the present study is to investigate the load-following capabilities of a hybrid nuclear-solar power plant and to find the optimal TES capacity and the most profitable operation strategy of the hybrid system for a specific geographical location. The TES sizing and optimization of the hybrid power plant operation strategy are performed to maximize profitability based on historical hourly Direct Normal Irradiance (DNI) data and hourly wholesale electricity prices in Duqm, Oman. In Section 2, the hybrid system, the costing method, and the modelling and optimization approaches are briefly described. The thermodynamic evaluations of the hybrid system at different loads as well as the optimal TES size and the economic assessment results are presented in Section 3. Finally, the key findings from this study are summarized in the Conclusions, in Section 4.

2. Model design

2.1. Proposed hybrid nuclear-solar system

The schematic of the analysed hybrid nuclear-solar power plant is illustrated in Fig. 1. The hybrid system consists of four main blocks which are: the nuclear power block that generates heat from nuclear fission, the solar power block that absorbs concentrated solar rays from the sun, the thermal energy block that stores energy in form of heat, and the power generation block that contains all heat-to-power conversion components. The integration allows saturated steam exiting the steam generator to be superheated and reheated again using indirect solar heat through the TES system.

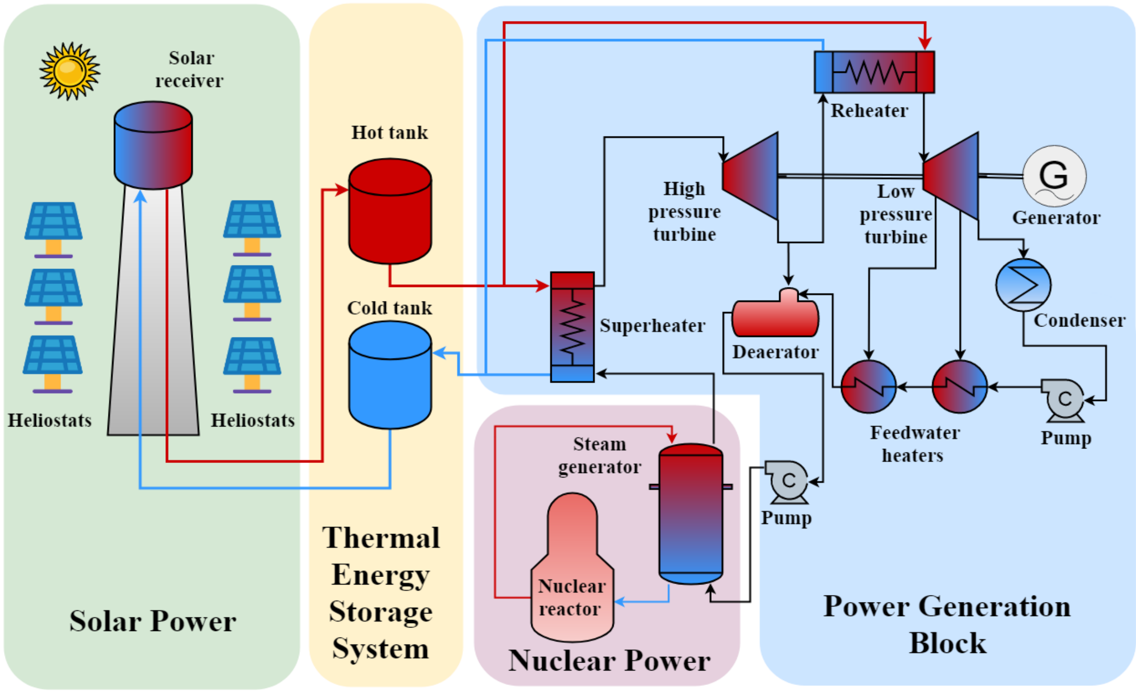

Fig. 1. Layout of the proposed hybrid nuclear-solar power plant integrated with TES system.

2.1.1. Nuclear power

Nuclear power plays a significant role in the hybrid system since it provides the majority of heat input in the power cycle. The selected nuclear power plant for this study is NuScale, which is a small modular reactor (pressurized light water reactor) designed by NuScale Power LLC. NuScale is still in the licensing process and is expected to be certified by US Nuclear Regulatory Commission in 2021 [17]. Table 1 summarizes the key parameters of a one-module NuScale power generation block.

Table 1. Main thermodynamic parameters of NuScale small modular reactor [17].

Parameter	Value
Reactor thermal power input (MWt)	160
Feedwater temperature (°C)	149
Feedwater pressure (kPa)	3410
Live steam mass flow rate (kg/s)	67.2
Steam generator outlet temperature (°C)	306
Steam generator outlet pressure (kPa)	3100

2.1.2. Solar power

Solar energy is utilized to superheat the slightly superheated steam outflowing from the steam generator as well as to reheat the steam exiting the high-pressure steam turbine. Superheating and reheating are performed to enhance the overall heat to power conversion efficiency and to increase the output power. In this study, solar tower technology is selected due to its capability to deliver high temperature heat which can reach up to 575 °C [18]. The selected heat transfer fluid of the solar system is molten-salt due to two reasons. Firstly, there are various molten salt types that are physically compatible to work at high temperatures range. Secondly, molten salt is suitable to be stored at high temperature, which has been already in use in many commercial CSP plants. Table 2 summarizes the key parameters of the solar power block used in this study, which has been optimized for the required heat input (i.e., including heat delivered to thermal storage) using System Advisor Model® (SAM) software, provided by National Renewable Energy Laboratory (NREL) [19]. The solar section parameters have been optimized in order to provide sufficient heat to superheat and then to reheat steam to 550 °C, which is supplied at the inlets of the high-pressure and low-pressure turbines.

Table 2. Key solar tower concentrated solar power block parameters and optimized dimensions [19].

Parameter	Value
Receiver inlet temperature (°C)	565
Receiver outlet temperature (°C)	260
Design solar multiple (-)	2.4
Design DNI (W/m^2)	950
Reflective area (km^2)	0.36
Receiver height (m)	110
Receiver area (m^2)	310

2.1.3. Thermal energy storage

Many TES options are available for CSP plants, such as molten salts, phase change materials, solid materials (e.g., concrete, bricks), and steam accumulation (commonly used in direct steam generation CSP plants) [20,21]. In this study, an indirect two-tank molten-salt plant is selected. Molten salt flows from the cold tank (T_c = 260 °C), is heated by solar energy during the daytime, and then stored in the hot tank (T_h = 565 °C). The selected molten salt is 40 wt% $NaNO_3$ + 40 wt% KNO_3 due to its capability to withstand the specified temperature range [22]. The heated molten salt is then used for heat addition in the superheater and the reheater whenever it is needed. The TES capacity is an independent variable in this model, and is optimized to maximize profitability, as described in Section 2.3.2.

2.1.4. Power generation block

A steam Rankine cycle is used for power generation in the hybrid system. The power generation block consists of the following key components: a superheater, a reheater, a high-pressure turbine, a low-pressure turbine, a condenser, two closed feedwater heaters, two pumps, a deaerator, and a generator. All power cycle components are sized based on the nominal load. The power cycle model details are indicated in Table 3. The model simulations are performed using MATLAB and all steam properties are obtained using REFPROP [23]. The live steam mass flow rate exiting the nuclear-powered steam generator and the outlet steam parameters of the solar superheater and the reheater are calculated using:

$$\dot{Q}_{\text{in}} = \dot{m}\,(h_{\text{out}} - h_{\text{in}}) \tag{1}$$

where $\dot{Q}_{\text{in}}$ is the (rate of) added heat, $\dot{m}$ the mass flow rate, h the enthalpy of steam, and subscripts 'in' and 'out' indicate the conditions at the inlet and the outlet of the component.

Equations (2-5) are used to calculate the generated power by the turbines and needed by the pumps:

$$\dot{W}_{\text{T}} = \dot{m}\,(h_{\text{in}} - h_{\text{out}}) \tag{2}$$

$$\eta_{\text{T}} = \frac{(h_{\text{in}} - h_{\text{out}})}{(h_{\text{in}} - h_{\text{out,is}})} \tag{3}$$

$$\dot{W}_{\text{P}} = \dot{m}\,(h_{\text{out}} - h_{\text{in}}) \tag{4}$$

$$\eta_{\text{P}} = \frac{(h_{\text{out,is}} - h_{\text{in}})}{(h_{\text{out,}} - h_{\text{in}})} \tag{5}$$

with $\dot{W}_{\text{T}}$ and η_{T} the turbine power and isentropic efficiency, $\dot{W}_{\text{P}}$ and η_{P} the pump power and isentropic efficiency, and subscript 'is' indicates properties evaluated at equivalent isentropic conditions.

The plant's net generated power and net thermal efficiency are calculated from:

$$\dot{W}_{\text{net}} = (\eta_{\text{Gen}} \sum \dot{W}_{\text{T}}) - \sum \dot{W}_{\text{P}} \tag{6}$$

$$\eta_{\text{Cycle}} = \frac{\dot{W}_{\text{net}}}{\dot{Q}_{\text{SMR}} + \dot{Q}_{\text{CSP}}} \tag{7}$$

where η_{Gen} is the generator efficiency, $\dot{Q}_{\text{SMR}}$ and $\dot{Q}_{\text{CSP}}$ the nuclear and solar heat rate additions.

Table 3. Main assumptions and full load power steam cycle parameters.

Parameter	**Value**	**Reference**
HPT inlet temperature (°C)	550	Assumed
HPT inlet pressure (kPa)	3040	[12]
Average HPT full load isentropic efficiency (%)	90	[12]
LPT inlet temperature (°C)	550	Assumed
LPT inlet pressure (kPa)	525	Optimized
Average LPT full load isentropic efficiency (%)	92	[12]
Condenser pressure (kPa)	8.5	[24]
Pump isentropic efficiency (%)	88	[12]
Generator mechanical efficiency (%)	98	[11]

Part-load operation is performed by varying the amount of heat added in the solar power superheater and the reheater. For example, if the system is requested to operate at 80% load, the amount of heat provided in the superheater or the reheater is reduced, which results in lower turbine inlet temperature, thus, less amount of electricity generated. For sake of simplicity, the turbine bleeding pressure are kept constant. However, the steam cycle model accounts for part-load turbine efficiency using [25]:

$$\eta_{\mathrm{i}} = \eta_{\mathrm{i}}^{\mathrm{D}} - 2\left(\frac{N\sqrt{\Delta h_{\mathrm{s}}^{\mathrm{D}}}}{N^{\mathrm{D}}\sqrt{\Delta h_{\mathrm{s}}}} - 1\right)^2 \quad (8)$$

where η_{i} is the turbine isentropic efficiency, N the shaft rotational speed, Δh_s the equivalent isentropic enthalpy change across the turbine, and superscript 'D' indicates the design point conditions.

It is assumed that the shaft speed is constant for all loads as being connected a fixed power grid frequency, typically 50 or 60 Hz depending on the country's electricity grid.

2.2. Cost estimation

Table 4 summarizes the relations used for determining the overall cost of the hybrid system. The solar power block cost correlations were extracted from NREL reports and SAM [19,26]. In the nuclear power block, the costs are based on available data with power generation components excluded. The capital indirect cost accounts for installation costs, safety, etc. The annual operation and maintenance (O&M) cost is taken as 3% of the capital cost. The main variation in the TES sizing is the cost of the TES system. The TES cost correlation is nonlinear as it depends on the size of the molten-salt tanks that are cylindrical. Hence, the surface area of the tanks (i.e., amount of material) increases nonlinearly with the tank volume.

The Levelized Cost of Electricity (LCOE) is calculated from:

$$LCOE = \frac{\sum_{t=1}^{n} \frac{C_t + O\&M_t + F_t}{(1+r)^t}}{\sum_{t=1}^{n} \frac{E_t}{(1+r)^t}} \quad (9)$$

where C_t is the capital cost in year 1, $O\&M_t$ is the operation and maintenance expenditure in year t, F_t the fuel expenditure in year t, E_t the electricity generation in year t, r the discount rate, and n the life of the system. In this study, all analyses are performed based on a 25-year lifetime with a discount rate of 7% and a power plant availability factor of 0.9.

The net profit is calculated from:

$$Net\ Profit = \sum_{t=1}^{n} \frac{I_t}{(1+r)^t} - \sum_{t=1}^{n} \frac{C_t + O\&M_t + F_t}{(1+r)^t} \quad (10)$$

$$I_t = \sum_{i=1}^{8760} EP(i)P(i) \quad (11)$$

where I_t is the annual income, $EP(i)$ the electricity price of hour i, and $P(i)$ the power generated at time (hour) i. It should be noted that no subsidies have been assumed for the renewable electricity generation.

All costing and economic analyses in this work are based on US$ as the currency. CAPEX figures include engineering and building costs, but do not include land costs.

Table 4. *Hybrid nuclear-solar power plant costs.*

Components and costs	Costing parameter	Cost ($)
Solar power block		
Solar tower [26]	Tower height (m)	$1835\ H^2 - 285868\ H + 3000000$
Receivers [19]	Receiver area (m^2)	$103000000\ (A_{\mathrm{RC}}/1571)^{0.7}$
Heliostat field [19]	Reflective area (m^2)	$156\ A_{\mathrm{RF}}$
Nuclear power block		
Reactor island [27]	Electrical power (kWe)	$4070\ P_{\mathrm{Nuc}}$
Nuclear fuel [28]	Nuclear thermal energy (MWht)	$5.76\ E_{\mathrm{Nuc}}$
Energy storage block [16,22,29,30]	Storage capacity (kWht)	$32.6\ (C_{\mathrm{TES}})^{0.915}$
Power generation block [19]	Gross electrical power (kWe)	$1330\ P_{\mathrm{Gnr}}$
Land [19]	Land area (m^2)	$2.47\ A_{\mathrm{L}}$
Capital indirect	Capital direct costs ($)	10% of direct cost
Fixed O&M per year	Total capital costs ($)	3% of total capital costs

2.3 Optimization

Optimization is performed in two steps: (1) the selected steam cycle operating variables are optimized to achieve maximum efficiency at different solar/nuclear input ratios, (2) the TES capacity is optimized to achieve maximum system profitability. Details of the two-step approach are provided below.

2.3.1. Steam cycle thermal efficiency optimization

The first step aims to maximize the heat-to-electricity conversion efficiency of the hybrid system. This is based on the comparison of the full-rated power output and the cycle thermal efficiency of the hybrid system vs a standalone nuclear reactor. Once all steam cycle parameters (i.e., steam flow rate, temperature, pressure) are calculated and verified, the thermal efficiency optimization process then starts. The generated results specify the steam cycle variables (i.e., turbine bleed pressure and mass flow rate, feedwater pump outlet pressure, etc.) that give maximum cycle efficiency for full load under specified technical constraints. The first step optimization problem is expressed as:

$$\max_{\dot{m}_{\mathrm{TB1}},\dot{m}_{\mathrm{TB2}},\dot{m}_{\mathrm{TB3}},T_{\mathrm{SH}},T_{\mathrm{RH}}}\{\eta_{\mathrm{Cycle}}^{\mathrm{Load}}\} \tag{12}$$

where $\eta_{\mathrm{Cycle}}^{\mathrm{Load}}$ cycle is the thermal to electrical efficiency, $\dot{m}_{\mathrm{TB1}}, \dot{m}_{\mathrm{TB2}}, \dot{m}_{\mathrm{TB3}}$ are the turbine bleeds mass flow rate, respectively, T_{SH} and T_{RH} the superheater and reheater outlet temperatures, respectively. It is noted that all system components are designed and sized for full-load operation. Efficiency optimization is also performed for part-load operation (from 55% to 100%). The optimized efficiency is then plotted against the part-load to generate a correlation that is then implemented in the TES sizing optimization model. All optimization tasks are solved using MATLAB's non-convex interior point algorithm *fmincon* or genetic algorithm function *ga* that satisfies a defined set of non-linear constraints.

2.3.2. TES capacity optimization

TES capacity optimization is performed with the main objective of maximizing profitability. The main optimization function inputs are the historic data of the wholesale electricity price of a specific region and the historic data of direct normal irradiance in the same region. The optimization is conducted assuming that all inputs data are the same for the entire lifetime of the hybrid system. Figure 2 shows the schematic of the TES size and operation optimization task used in this study.

The TES sizing and operation strategy optimization problem is expressed as:

$$\max_{Q_{\mathrm{TES}},P_{\mathrm{out}}(t)}\{Net\ Profit\} \tag{13}$$

where Q_{TES} is the storage capacity, and $P_{\mathrm{out}}(t)$ the output power at time t (i.e., from 1 to 8760 h), which ranges from minimum to maximum percent (%) load.

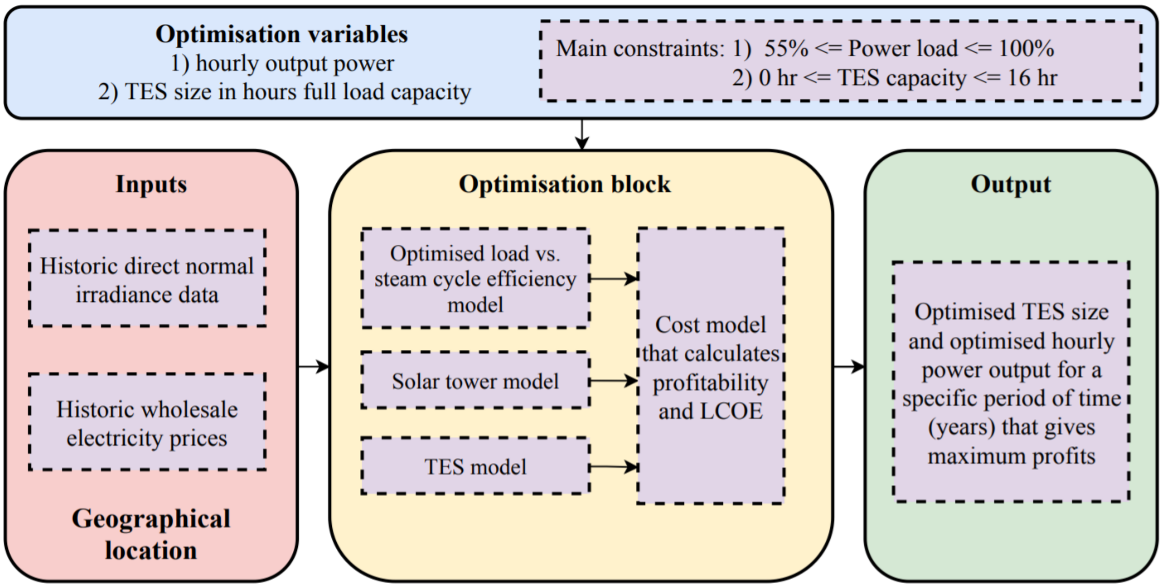

Fig. 2. Schematics of modelling approach and optimization function inputs and outputs.

2.3.3. DNI and electricity prices

In order to perform the simulations, input of hourly DNI data and wholesale electricity prices are required. Duqm, which is a city in Oman, was selected as the location of this power plant. DNI data have been extracted from European Commission's Photovoltaic Geographical Information System (PVGIS) [31]. In Oman, the Authority for Electricity Regulation (AER) has set a structured wholesale electricity price system (i.e., bulk supply charges) which is composed of four price levels :1) off-peak, 2) night-peak, 3) weekday day-peak, and 4) weekend day-peak. These prices vary depending on the month. Figure 3 indicates the electricity prices and their occurrences (number of hours) in Oman for the year of 2018 [32].The peak prices can reach up to 168 $/MWh during summer day time.

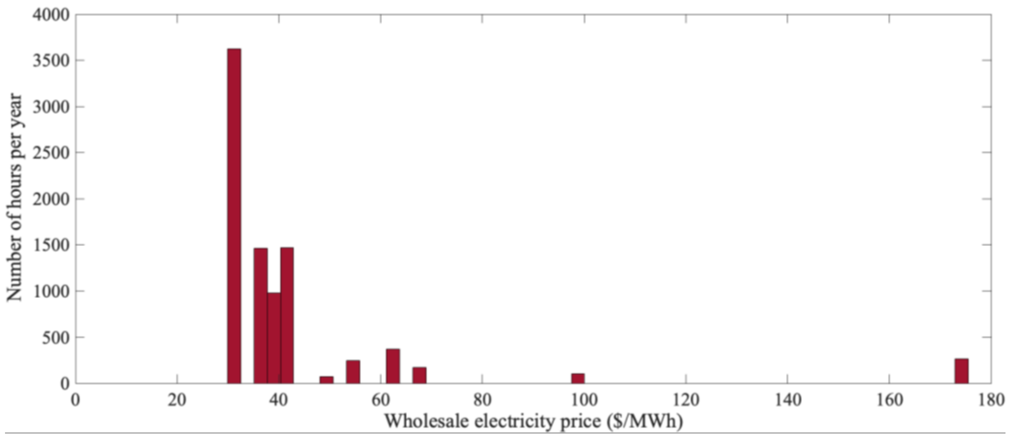

Fig. 3. Electricity prices and their occurrences (number of hours) in Oman in 2018 [32].

3. Results

3.1. Thermodynamic analysis

Table 5 summarizes the optimization analysis results of the hybrid system at different loads, compared to a standalone NuScale SMR. The hybridization concept increases the output power for full-load operation by 78%, from 50 MWe to 90 MWe. This increase is a result of increasing the total heat addition in the cycle. Moreover, the cycle thermal efficiency increases by 25%, from 31% to 39%, as a result of increasing the temperature of heat addition (i.e., adding a superheater and a reheater). The solar heat to electrical efficiency, calculated from Eq. (14), is about 56%, which is significantly high when compared to conventional CSP plants. This high efficiency level is very competitive to current efficiency levels of the combined cycle gas turbine plants, which is usually between 45-60%. Furthermore, the amount of thermal power needed to generate the extra 40 MW of electrical power is only 71 MWt, about 44% of the total nuclear heat input. This is calculated using Eq. (15).

$$\eta_{\mathrm{CSPtoEP}} = \frac{\dot{W}_{\mathrm{net}} - \dot{W}_{\mathrm{SMR}}}{\dot{Q}_{\mathrm{CSP}}} \tag{14}$$

$$\dot{Q}_{\mathrm{ratio}} = \frac{\dot{Q}_{\mathrm{CSP}}}{\dot{Q}_{\mathrm{SMR}}} \tag{15}$$

Overall, the predicted performance of the hybrid system reveals improvements over conventional nuclear technology, which can make the former a competitive technology relative to the most efficient conventional power plants. At 55% part-load operation, the net electrical power is less than 50 MWe since the hybrid system operates using nuclear heat only and power cycle components that are designed for full-load operation. Thus, it is expected to have relatively greater heat and mechanical losses, especially in heat exchangers and turbines, at low-load operation scenarios.

Table 5. Thermodynamic analysis results of the hybrid nuclear-solar system (HNS) compared to a standalone small modular nuclear reactor (one unit of NuScale), considering HNS plants at full load (100%), 75% part load and 55% part load (technical min output, with no solar input to the system).

Parameter	**NuScale [20]**	**HNS (100 %)**	**HNS (75 %)**	**HNS (55 %)**
Net electrical power (MWe)	50	90	67	48.9
Incremental power (MWe)	NA	40	17	-1.1
Nuclear thermal power input (MWt)	160	160	160	160
Solar thermal power input (MWt)	0	71	32	0
Total thermal power input (MWt)	160	230	190	160
Power block net efficiency (%)	31	39	35	30.8
Solar heat to electrical efficiency (%)	N/A	55	53	0
Solar heat to nuclear heat ratio (%)	N/A	44	20	0

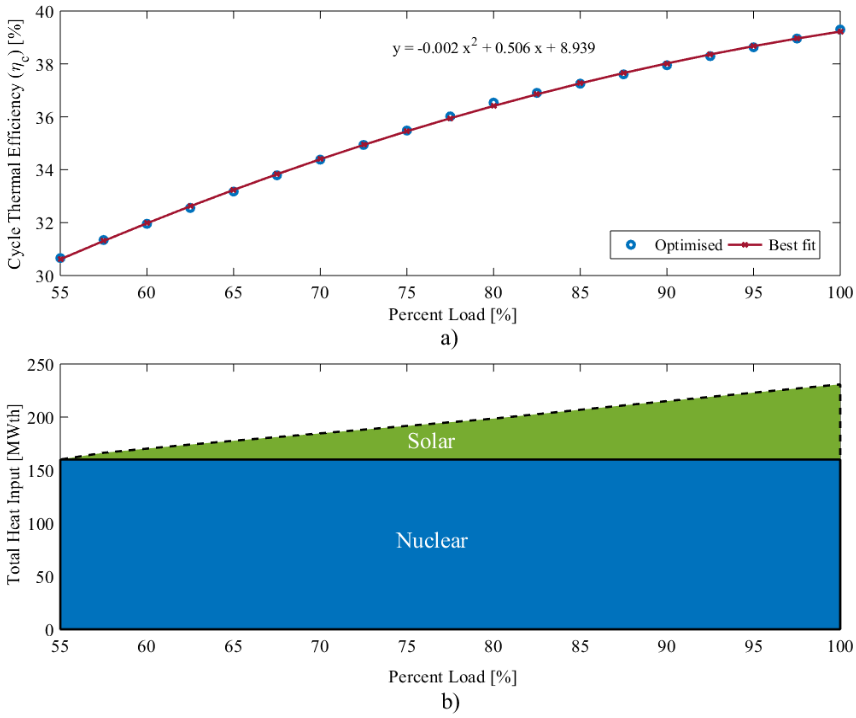

Fig. 4. a) Optimized cycle electrical efficiency of the hybrid system at each output power rate (55% to 100%) with its corresponding best fit function, and b) indication of the amount of nuclear and solar heat addition for each percent of nominal output power.

In order to move to the next step (i.e., TES capacity optimization), the total thermal-electrical efficiency is optimized for each load at 2.5% increments (from 55% to 100%). The optimization function calculates the steam cycle variables (i.e., superheater and reheater outlet temperature, turbine bleeds mass flow rates) that maximize efficiency. The optimized efficiency is plotted against percent load as indicated in Fig. 4 (a) with a best fit function that is used for the TES capacity optimization. The correlation is presented in Eq. (16) and Q_{CSP} is calculated using equation Eq. (7):

$$\eta_{\mathrm{Cycle}}\,(\%) = -0.002\,[Load(\%)]^2 + 0.506\,[Load(\%)] + 8.939 \qquad (16)$$

The amount of heat addition for each load is indicated in Fig. 4 (b). The amount of nuclear heat is always constant at 160 MWt whereas total power output is modulated by varying the amount of solar heat addition. This explains why load following is constrained between 55% and 100% of the full load.

3.2. TES sizing and profitability analysis

The results of TES capacity optimization of the hybrid system, taking Oman as a location, are shown in Fig. 5 (a). The results show that the maximum profit can be obtained at a TES capacity corresponding to 11 h of full-load operation. After this time, the profits start decreasing as the cost of increasing TES capacity is higher than the income of selling electrical power. The obtained LCOE is 78 $/MWh, which is comparable to nuclear only LCOE (65-100 $/MWh) and lower than a standalone CSP plant (100-180 $/MWh) [27,33].The relatively low LCOE is reasonable due to the assumptions that no land cost is considered in the cost assessment as well as the high availability factor of the hybrid system.

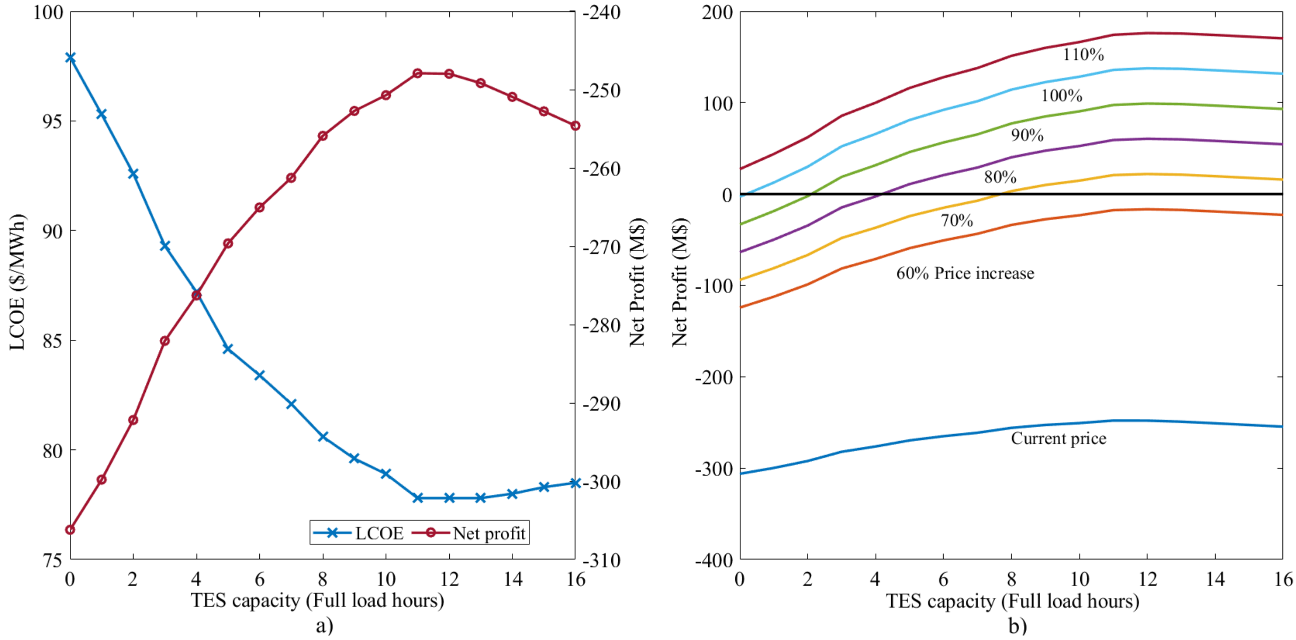

Fig. 5. a) LCOE and the net profit for different TES capacities, and b) net profit at different TES capacities for different electricity price scenarios.

Although the hybrid system is operating close to full load for the entire 25 years with an availability factor of 90%, the profits are still negative (-248 M$). This arises from the low wholesale electricity prices in Oman (43 $/MWh average) as compared to other countries (e.g., 74 $/MWh average in the UK in 2018) [32,34]. Figure 5 (b) shows the profit returns with respect to the TES storage size at different electricity price increase scenarios. It can be clearly seen that in order to make this particular hybrid system economically viable in Oman, the average electricity price should increase by at least 70%, to UK levels, with an 8 h of TES capacity. Moreover, in the case of no storage, it is only possible to make profits when the electricity price is doubled. Table 6 summarizes the costs of the optimized hybrid power plant with a TES capacity of 11 h for different electricity prices increase scenarios.

Table 6. Summary of costs and economics of the hybrid power plant with the optimized TES capacity of 11 h for different electricity price scenarios.

Obtained costs	**Value**	**Other parameters**	**Value**
Total capital cost (M$)	471	Total power generated per year (GWh)	770
Nuclear power block (M$)	204	Total income for 25 years (M$)	384
Solar power block (M$)	134	Total expenditure for 25 years (M$)	632
Power generation block (M$)	118	Total profits (M$)	-248
TES system – 11 h (M$)	16	70% price increase (M$)	21
O&M costs (M$)	14	100% price increase (M$)	138
Fuel cost (M$)	2	LCOE ($/MWh)	78

Figure 6 shows: (a) the hourly power output on the left axis label and its respective electricity price on the right axis label, (b) the thermal energy stored, and (c) and the rate of thermal energy input (i.e., nuclear to cycle, solar to cycle, solar to TES, and TES to cycle) for the optimized hybrid system of over one year (represented as a weekday and a weekend day per month). At peak electricity prices, from May to September, the system generates maximum power whenever it is possible to make higher profits. There are some hours in July and August, from 300 to 380 h in Fig. 6 (a), where it operates at lower loads since the TES capacity is limited. However, the system behaves in a way that guarantees maximum power is delivered at the peak hours of the day. The system could possibly operate at full load for the entire year. However, the cost of adding extra storage capacity (i.e., more than 11 h) is higher than the revenues made from selling electricity at the current price levels.

Overall, the hybrid system shows its capabilities of generating flexible and clean electrical power at competitive LCOE and it could be an economically viable option in cities where the wholesale electricity price averages are higher than the current average price in Oman.

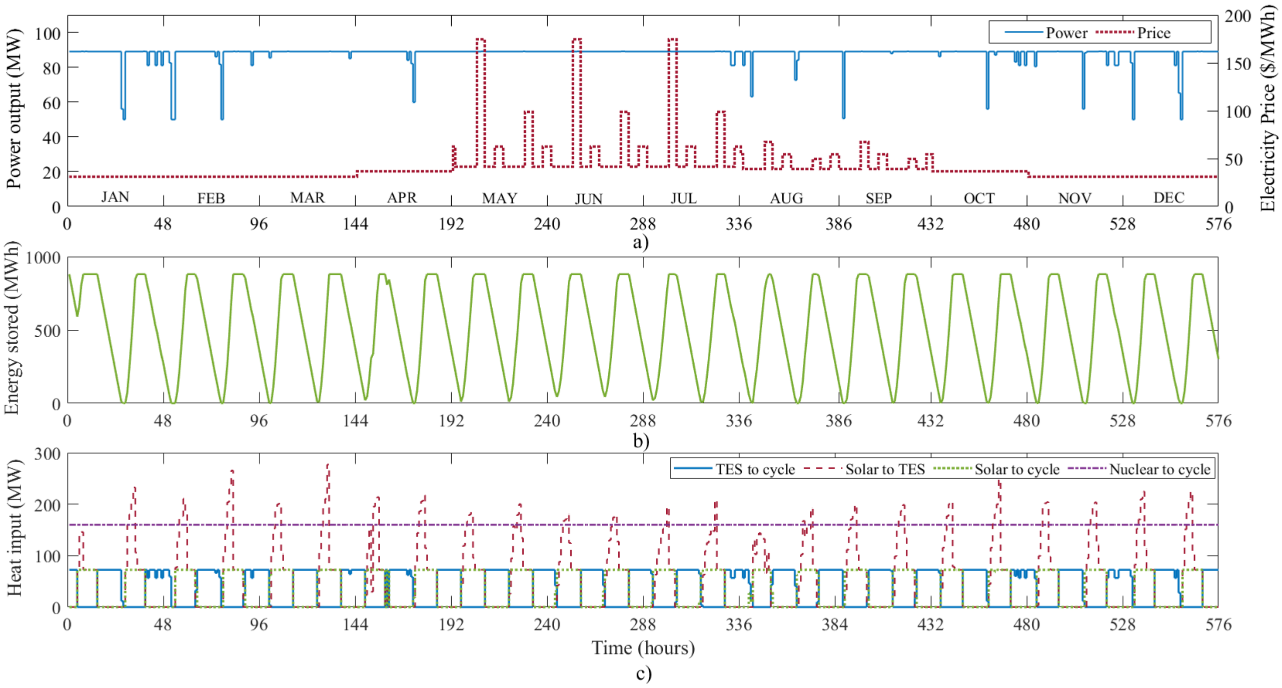

Fig. 6. a) Power output and the corresponding electricity price for two days a month (a weekday and a weekend) for one year, b) the amount of stored energy in the optimized TES size, and c) nuclear and solar heat inputs to the cycle or to the TES system.

4. Conclusion

This paper presents a thermodynamic analysis of a 90-MWe hybrid, combined nuclear-solar power plant integrated with a thermal energy storage system during both full-load and part-load operation. It identifies the optimal thermal-store size and the operational strategy that maximizes profits. Duqm, a city in Oman, is selected as the location for the proposed hybrid power plant. The modelling and optimization framework presented here enables a comparison of the thermodynamic performance of the hybrid system against a standalone nuclear reactor, also during load following operations. For the thermal-store size optimization, a detailed cost model was developed and optimized to calculate the expected levelized cost of electricity and profits of the system installed and operated in Duqm.

Performance predictions show that the overall hybrid-system efficiency and solar heat-to-power efficiency of the proposed system have the potential to reach values as high as 36% and 56%, respectively, at full load. Moreover, the hybrid system can deliver flexible power ranging from 55% to 100% of its rated power, while the nuclear reactor operates at its full rated power. Additionally, the optimal thermal storage capacity for the studied case is 11 h bringing the levelized cost to about 78 $/MWh, which is considered very competitive relative conventional plants.

The study, therefore, concludes that such a hybrid system is promising, even though an installation in Oman is not economically viable at present, given the low wholesale electricity prices in Oman (43 $/MWh average vs. 74 $/MWh in the UK in 2018). Nevertheless, the technology can become viable if electricity tariffs increase by 70% to UK levels. This price increase is not far from future projections, since Oman currently depends largely on natural gas for electricity generation, which is comparatively cheap at the current oil and gas prices, and therefore is expected to increase.

Future work will include improvements to the steam cycle model for part-load operation predictions and to the cost modelling and methods, e.g. by considering a multitude of correlations, as well as considerations of alternative hybrid configurations, thermal storage options, and operational scenarios and geographical locations, especially where such a technology will be particularly competitive.

Acknowledgement

This work was supported by the UK Engineering and Physical Sciences Research Council (EPSRC) [grant numbers EP/P004709/1, EP/S032622/1, EP/R045518/1]; and the Department for International Development (DFID) through the Royal Society-DFID Africa Capacity Building Initiative. Data supporting this publication can be obtained on request from cep-lab@imperial.ac.uk.

References

[1] IAEA, Advances in small modular reactor technology developments. 2018 Edition; 2018.
[2] Honorio L., Bartaire J.G., Bauerschmidt R., Ohman T., et al., Efficiency in electricity generation. Technical Report No.: 2003-030-0548, Union of the Electricity Industry, EURELECTRIC, Brussels, Belgium; 2003.
[3] Masters G.M., Renewable and efficient electric power systems. John Wiley, New Jersey, USA; 2004.
[4] Ruth M.F., Zinaman O.R., Antkowiak M., Boardman R.D., et al., Nuclear-renewable hybrid energy systems: Opportunities, interconnections, and needs. Energy Conversion and Management 2014;78:684–694.
[5] Garcia H.E., Mohanty A., Lin W.C., Cherry R.S., Dynamic analysis of hybrid energy systems under flexible operation and variable renewable generation-Part I: Dynamic performance analysis. Energy 2013; 52:1–16.
[6] Garcia H.E., Mohanty A., Lin W.C., Cherry R.S., Dynamic analysis of hybrid energy systems under flexible operation and variable renewable generation-Part II: Dynamic cost analysis. Energy 2013;52:17–26.
[7] Suman A., Hybrid nuclear-renewable energy systems: A review. Journal of Cleaner Production 2018;181:166–177.
[8] Kuravi S., Goswami Y., Stefanakos E.K., Ram M., et al., Thermal energy storage for concentrating solar power plants. Technology and Innovation 2012;14:81–91.
[9] Pantaleo A.M., Camporeale S.M., Miliozzi A., Russo V., et al., Thermo-economic assessment of an externally fired hybrid CSP/biomass gas turbine and organic Rankine combined cycle. In: Proceedings of the 8th International Conference on Applied Energy (ICAE), Beijing, China; 8-11 Oct. 2016.

[10] Pantaleo A.M., Camporeale S.M., Sorrentino A., Miliozzi A., et al., Hybrid solar-biomass combined Brayton/organic Rankine-cycle plants integrated with thermal storage: Techno-economic feasibility in selected Mediterranean areas. Renewable Energy 2020;147:2913-2931.
[11] Popov D., Borissova A., Innovative configuration of a hybrid nuclear-parabolic trough solar power plant. International Journal of Sustainable Energy 2018;37:616–639.
[12] Popov D., Borissova A., Innovative configuration of a hybrid nuclear-solar tower power plant. Energy 2017;125:736–746.
[13] Casella F., Casati E., Colonna P., Optimal operation of solar tower plants with thermal storage for system design. In: Proceedings of the 19th World Congress the International Federation of Automatic Control (IFAC), Cape Town, South Africa; 24-29 Aug. 2014.
[14] Guedez R., Topel M., Conde I., Ferragut F., et al., A methodology for determining optimum solar tower plant configurations and operating strategies to maximize profits based on hourly electricity market prices and tariffs. Journal of Solar Energy Engineering 2016;138:1–12.
[15] Zhuang X., Xu X., Liu W., Xu W., LCOE analysis of tower concentrating solar power plants using different molten-salts for thermal energy storage in China. Energies 2019;12:1–17.
[16] Parrado C., Marzo A., Fuentealba E., Fernández A.G., 2050 LCOE improvement using new molten salts for thermal energy storage in CSP plants. Renewable and Sustainable Energy Reviews 2015;57:505–514.
[17] NuScale Power, Nuscale power. Available at: <www.nuscalepower.com/technology/licensing> [accessed: 9.1.2020].
[18] Islam M.T., Huda N., Abdullah A.B., Saidur R., A comprehensive review of state-of-the-art concentrating solar power (CSP) technologies: Current status and research trends. Renewable and Sustainable Energy Reviews 2018;91:987–1018.
[19] NREL, System advisor model (SAM). Available at: <https://sam.nrel.gov> [accessed: 2.12.2019].
[20] Dirker J., Juggurnath D., Kaya A. Osowade E. A., et al., Thermal energy processes in direct steam generation solar systems: Boiling, condensation and energy storage – A review. Frontiers in Energy Research 2019;6:1–35.
[21] Al Kindi A.A., Pantaleo A.M., Wang K., Markides C.N., Thermodynamic assessment of steam-accumulation thermal energy storage in concentrating solar power plants. Proceedings of the 11th International Conference on Applied Energy (ICAE), Vasteras, Sweden; 12-15 Aug. 2019.
[22] Ushak S., Fernández A. G., Grageda M., Using molten salts and other liquid sensible storage media in thermal energy storage (TES) systems. Advances in Thermal Energy Storage Systems 2015; 49–63.
[23] Lemmon E.W., Bell I.H., Huber M.L., McLinden M.O., NIST Standard reference database 23: Reference fluid thermodynamic and transport properties-REFPROP. Version 9.0; 2018.
[24] NuScale Power, Chapter ten: Steam and power conversion system. Part 2, Tier 2; 2018.
[25] Grote W., Ein Beitrag zur modellbasierten regelung von entnahmedampfturbinen. Dissertation, Ruhr-Universität, Bochum, Germany; 2009.
[26] NREL, Power tower plant cost and material input to life cycle assessment (LCA). Technical Report No.: NREL-8-ME-REP-0002 Rev. 2, Colorado, USA; 2012.
[27] World Nuclear Association, Economics of nuclear power. Available at: <www.world-nuclear.org/information-library/economic-aspects/economics-of-nuclear-power.aspx> [accessed 12.1.2020].
[28] Pannier C.P., Škoda R., Small modular reactor and large nuclear reactor fuel cost comparison. Energy and Power Engineering 2014;6:82–94.
[29] US DOE, Molten salt – Concept definition and capital cost estimate. Technical Report No. B&V File No. 40.1200; 2016.
[30] Glatzmaier G., Developing a cost model and methodology to estimate capital costs for thermal energy storage. Technical Report No.: NREL/TP-5500-53066, NREL, Colorado, USA; 2011.
[31] European Commission, Photovoltaic geographical information system. Available at: <https://re.jrc.ec.europa.eu/pvg_tools/en/tools.html#TMY> [accessed: 6.6.2020].
[32] Muscat Electricity Distribution Company, Cost reflective tariff (CRT). Muscat, Oman; 2018.
[33] IRENA, Renewable energy technologies: Cost analysis series. Technical Report, Volume 1: Power Sector Issue 2/5, Abu Dhabi, UAE; 2012.
[34] NORD POOL, Historical market data. Available at: <www.nordpoolgroup.com/historical-market-data> [accessed 14.1.2020].